INTERACTION OF CYCLOMETALLATED Ru(II) DRUGS WITH GLUTATHIONE

HONORS RESEARCH THESIS

Presented in partial fulfillment of the requirements for graduation with *Honors Research Distinction* in the College of Arts and Sciences at The Ohio State University

By

Olivia M. Chen

Undergraduate Program in Molecular Genetics

The Ohio State University

May 2013

Thesis Committee:

Professor Claudia Turro, Advisor

Professor Terry Gustafson

Professor Anil Pradhan

ABSTRACT

Photodynamic therapy (PDT) utilizing light to activate metal complexes has emerged as an alternative strategy of cancer treatment that imparts greater specificity of toxicity. In the realm of PDT, light-activated inorganic metal complexes that covalently bind DNA have come to the fore as potential anticancer therapies. The cyclometallated complex *cis*-$[Ru(phpy)(phen)(CH_3CN)_2]^+$ **(1:** $phpy^-$ = deprotonated 2-phenylpyridine, phen = 1,10-phenanthroline) was recently found to inhibit tumor growth in mice with fewer major side effects. Treatment of the human ovarian cancer cell line OVCAR-5 with **1**, resulted in a fourteen-fold increase in toxicity in irradiated conditions as compared to dark conditions. Despite this large photoinduced increase in toxicity of **1**, the photophysical properties as well as the photoactivating mechanism are not fully understood; hence, both have been investigated for complex **1** and for the analog *cis*-$[Ru(phpy)(bpy)(CH_3CN)_2]^+$ (**2:** bpy = 2,2´-bipyridine). Within the cell, there is the possibility of ligand exchange occurring in the presence of coordinating solvent and a large intracellular pool of reduced glutathione (GSH), therefore the possible role that GSH may play in facilitating the production of toxic species was explored for **1** and **2**. Both complexes **1** and **2** undergo ligand exchange in the presence of GSH in the dark. The observed cytotoxicity of **1** may be explained by both GSH-facilitated ligand dissociation and photo-induced ligand exchange.

DEDICATION

I would like to dedicate this work to my family.

ACKNOWLEDGEMENTS

I have many people to thank for sparking my interest in chemistry and for allowing me a meaningful research experience. I would like to thank Dr. Singer, Dr. Stambuli, and Dr. Pei for being fantastic chemistry professors whose classes I have truly enjoyed. I would like to thank Yujie Sun for introducing me to his research, and many thanks to my advisor Professor Claudia Turro for welcoming me into her research group and allowing me the opportunity to learn and explore my interest in science in an encouraging environment. Thank you Robert Garner and Alycia Palmer for your friendship, and for being always patient and encouraging mentors. I would also like to express my gratitude to The Ohio State University and its alumni for believing in and investing in undergraduate research; the numerous opportunities to take part in research symposiums and the generous scholarships that I have received have greatly supported my studies and enriched my undergraduate journey. I am both excited and grateful to have been a part of this research experience, which has encouraged my questions and nurtured my interest in research. I feel inspired by the generosity of the all those who have helped to make this possible. Thank you all!

VITA

July 2011 – August 2011……Research Associate, Brain Mind Institute,
École Polytechnique Fédérale de Lausanne

September 2011 – June 2012……..Research Associate, Department of Psychology and
Neuroscience, The Ohio State University

June 2012 – August 2012……Research Associate, Institute of Medical Biology
Agency for Science, Technology, and Research

September 2010 – May 2013……..…Undergraduate Teaching Assistant,
Department of Chemistry, The Ohio State University

August 2013……Undergraduate Research Scholarship,
The Ohio State University

December 2013……..Sigma Xi Grant in Aid of Research,
The Ohio State University

March 2013…….Natural and Mathematical Sciences Research Forum
Best Poster in Chemistry

May 2013……B.S. Molecular Genetics, The Ohio State University

PUBLICATIONS

Palmer, Alycia; Peña, Bruno; Sears, Bryan; **Chen, Olivia**; Thummel, Randall; Dunbar R., Kim; Turro, Claudia. "Cytotoxicity of Cyclometallated Ruthenium Complexes: The Role of Ligand Exchange on the Activity." *Philosophical Transactions of the Royal Society A. (Accepted July 2012).*

FIELD OF STUDY

Major Field: Molecular Genetics

Minor Fields: Chemistry, Spanish

LIST OF FIGURES

complexes to the DMSO-d_6:D_2O solution. (b) and (e) were measured after 20 h in the dark at room temperature. (c) and (f) were measured 20 min after 10 equivalents of GSH were added to the respective samples described in (b) and (e).

Figure 13. ESI-MS of **1** (670 μM) in DMSO-d_6:D_2O (33:67, v:v) (a) immediately after addition of 10 equivalents of GSH to **1** in the DMSO-d_6:D_2O solution (b) after 20 h in the dark at room temperature (c) after 30 min of irradiation ($\lambda > 455$ nm). ESI-MS. of **1** (670 μM) in DMSO-d_6:D_2O (33:67, v:v) (d) immediately after addition of 5 equivalents of GSSG to **1** in the DMSO-d_6:D_2O solution (e) after 20 h in the dark at room temperature (f) after 30 min of irradiation.

Figure 14. Irradiation of the DMSO-d_6-monosubstituted species $[Ru(phpy)(phen)(CH_3CN)(DMSO\text{-}d_6)]^+$ is thought to lead to isomerization of the DMSO molecule from S-bound to O-bound.

Figure 15. ESI-MS of **2** (665 μM) in DMSO:H_2O (33:67, v:v) (a) immediately after addition of 10 equivalents of GSH to **2** in the DMSO:H_2O solution (b) after 20 h in the dark at room temperature (c) after 30 min of irradiation ($\lambda > 455$ nm). ESI-MS of **2** (665 μM) in DMSO:H_2O (33:67, v:v) (d) immediately after addition of 5 equivalents of GSSG to **2** in the DMSO:H_2O solution (e) after 20 h in the dark at room temperature (f) after 30 min of irradiation.

TABLE OF CONTENTS

CHAPTER 1

INTRODUCTION

1.1 BACKGROUND

The anti-cancer agent cisplatin, *cis*-$Pt(NH_3)_2Cl_2$, is an inorganic metal complex that has been widely employed to treat a range of cancers, including ovarian and testicular malignancies. Cisplatin is thermally activated and covalently binds cellular DNA, inhibiting DNA replication among other cellular processes, which results in the death of tumor cells; however, the nonspecific thermal activation of cisplatin also leads to the death of healthy cells. Patients undergoing cisplatin treatment frequently experience side effects including altered hepatic functioning, neurotoxicity, nephrotoxicity, and weight loss.[1] Multiple attempts to treat recurrent tumors with cisplatin or prolonged treatment with cisplatin, are often unsuccessful due to the increased resistance of cancer cells to the drug.[17] These drawbacks of cisplatin have made other cancer treatments with greater specificity toward tumor cells a more attractive alternative.

In photochemical reactions, the absorption of a photon supplies the energy that excites a molecule from the ground state to the excited state. Excited molecules can drive chemical reactions that may not be accessible otherwise, such as the ligand exchange observed in many Ru(II) and Rh_2(II,II) compounds. When this occurs in the presence of coordinating solvent, photolabile ligands may be exchanged with surrounding solvent molecules. These photochemical reactions offer several practical advantages over thermally activated reactions, which occur at

ambient temperature. First, light energy can be used to overcome large energy of activation barriers to generate photoproducts. Second, utilizing light to initiate a chemical reaction enables restriction of the reaction and the generated products to a specific locale. This advantage of photoinduced reactions makes light-activated compounds particularly amenable to applications in many fields, including medicine.

The use of photoinitiated reactions in the medical field has emerged as a promising approach for treating microbial infections as well as malignant cancers.[2,3] The potential that photoactivated compounds hold as therapeutics has spurred the growth of the PDT field, especially with regard to treating cancer. Light-activated compounds used in photochemotherapy exhibit a relatively low level of toxicity in the dark, but a high level of toxicity once irradiated. The use of light to selectively activate the compound allows for the toxic effects to be localized to the region requiring treatment, for instance, the tumor site. This enhanced specificity of activation reduces the adverse side effects posed by treatment. An additional advantage in photochemotherapy lies in the less invasive nature of such treatments; the drug is administered intravenously and an endoscope is used to deliver light to the tumor site. These advantageous qualities of PDT have encouraged continued exploration of light-activated compounds for PDT cancer therapies.

1.2 PHOTODYNAMIC THERAPY AGENTS

There are several important qualities that should be considered in order to identify suitable PDT agents.[4] First, compounds should absorb light within the PDT window (600 – 850 nm). Low energy light within this visible to near-infrared range is not greatly absorbed by water

or biomolecules such as hemoglobin within the body and therefore provides the deepest tissue penetration by light. Second, photoactivation of the PDT agent should have a high quantum yield, which is a measure of the efficiency of the PDT agent in using light energy to generate the photoproduct. Third, the PDT agent must be relatively nontoxic in the dark, but upon selective irradiation the photoproducts should be toxic. Organic compounds exhibiting these qualities were some of the first FDA-approved PDT agents for chemotherapy.

Porfimer sodium, a hematoporphyrin derivative, has been used to treat a variety of cancers including esophageal, bladder, head, and neck cancers.[5] The drug is injected intravenously in the dark and is relatively nontoxic in this condition. After uptake by cells, the treatment site is irradiated with low energy light. The excited porfimer sodium molecules within this region transfer energy to surrounding triplet oxygen, thereby producing singlet oxygen, a reactive oxygen species (ROS) that causes cell damage and eventual cell death. The mechanism of action of Porfimer sodium is illustrated in **Figure 1**.

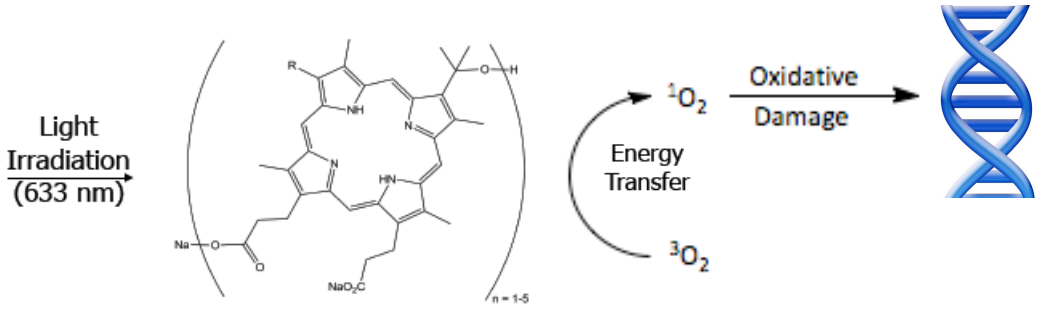

Figure 1. Low energy light excites porfimer sodium, which relaxes with concomitant production of a cell-damaging reactive oxygen species.

While organic PDT agents have proven useful in treating many different cancers, organic PDT compounds like Porfimer sodium require the presence of oxygen in the surrounding environment to generate tumor cell killing species, singlet oxygen, $^1O_2$; the latter produces reactive oxygen species (ROS). As a result, the utility of these organic PDT agents is limited to treating cancers found in well-oxygenated environments.[6,7] Unfortunately, many aggressive, malignant cancers exist in hypoxic surroundings.[6,7] As a result, PDT agents that can operate through oxygen-independent mechanisms are being explored as potential treatments against these hypoxic cancers. Several light-activated inorganic compounds have been shown to possess oxygen-independent cell-killing mechanisms among other desirable qualities for PDT agents.[8,9,10] Some of these photoactive inorganic compounds function like organic compounds and kill cells through the production of ROS, while others are activated by light to covalently bind to DNA through singular or dual-binding mechanisms.[9] DNA binding inhibits cellular processes including transcription and DNA replication, leading to eventual cell death. A better understanding of the photoactive mechanism and photophysical properties of these light-activated inorganic complexes is therefore important for advancing the development of a line of treatments effective against resilient, hypoxic cancers.

Of particular interest are light-activated inorganic compounds that readily bind DNA upon selective irradiation. This class of the light-activated inorganic compounds operates under a similar mechanism of action as the older chemotherapeutic drug cisplatin, *cis*-$[Pt(NH_3)_2Cl_2]$. Cisplatin was first identified as possessing chemotherapeutic properties in the 1970s. In the cell, the complex undergoes thermal activation and exchanges its two Cl^- ligands for water molecules. The intermediate complex *cis*-$[Pt(NH_3)_2(H_2O)Cl]^+$ is first formed, followed by formation of the activated bis-aqua complex *cis*-$[Pt(NH_3)_2(H_2O)_2]^{2+}$. Water forms weak bonds with Pt(II) and is

easily displaced, allowing Pt(II) to covalently bind to adjacent purine residues of DNA, forming 1,2-intrastrand adducts that cause the double helix to kink.[11] DNA repair machinery fails to repair this kinked DNA and affected cells cannot proliferate and instead induce cell death. The mode of action of cisplatin is illustrated in **Figure 2.**

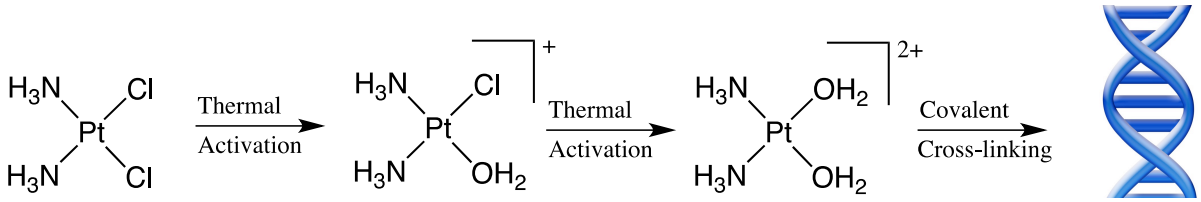

Figure 2. Thermal activation of Cisplatin leading to DNA binding.

Though cisplatin is an oxygen-independent chemotherapeutic agent that has been widely used to kill tumors, the complex is thermally activated and therefore lacks specificity for tumor cells. This is a major disadvantage that leads to serious side effects and damage to healthy tissue and rapidly dividing cells in the body. Despite this drawback, the DNA-binding mechanism of cisplatin can be a useful mechanism to attain cell death if the chemistry is able to be controlled, such as through the use of light. Therefore, compounds that can bind to DNA only when irradiated with light have been investigated for the development of inorganic light-activated PDT compounds that kill cells, but with greater specificity toward tumor cells. Light-activated inorganic complexes that operate similarly to cisplatin have been termed photo-cisplatin analogs. Two such photo-cisplatin analogs and are illustrated in **Figure 3** below.[12,9]

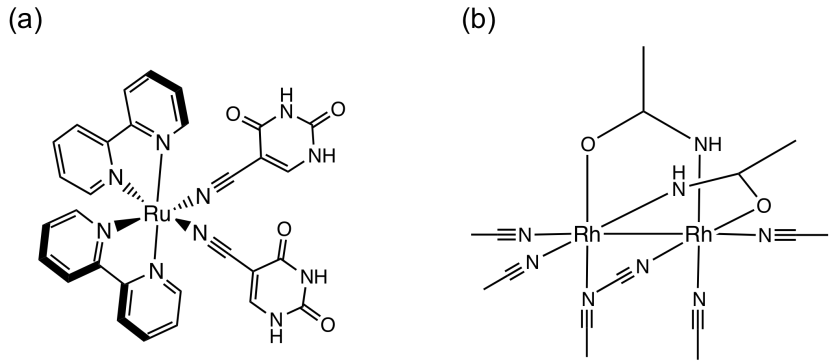

Figure 3. photo-cisplatin analogs (a) $[Ru(bpy)_2(5\text{-cyanouracil})_2]^{2+}$ (bpy = 2,2'-bipyridine) and (b) *cis*-H,T-$[Rh_2(HNOCCH_3)_2(CH_3CN)_6]^{2+}$.

1.3 RUTHENIUM(II) PHOTO-CISPLATIN ANALOGS

Photo-cisplatin analogs containing a ruthenium, instead of a platinum, metal center make up a group of promising inorganic PDT agents, with several ruthenium-based agents already in clinical trials.[13,14] A group of polypyridyl ruthenium (II) compounds of the form *cis*-$[Ru(bpy)_2(L)_2]^{2+}$ (bpy = 2,2'-bipyridine; L = NH_3, pyridine, or CH_3CN) has been shown to exhibit the desirable qualities of PDT agents. When irradiated with visible light, these complexes lose their photolabile ligands in exchange for the coordination of solvent water molecules. The activated bis-aqua species *cis*-$[Ru(bpy)_2(H_2O)_2]^{2+}$ then covalently binds to DNA in a mechanism similar to that of cisplatin.[10,15,16] These polypyridyl ruthenium compounds have therefore earned the title of photo-cisplatin analogs. See **Figure 4** for the mechanism of action of *cis*-$[Ru(bpy)_2(L)_2]^{2+}$.

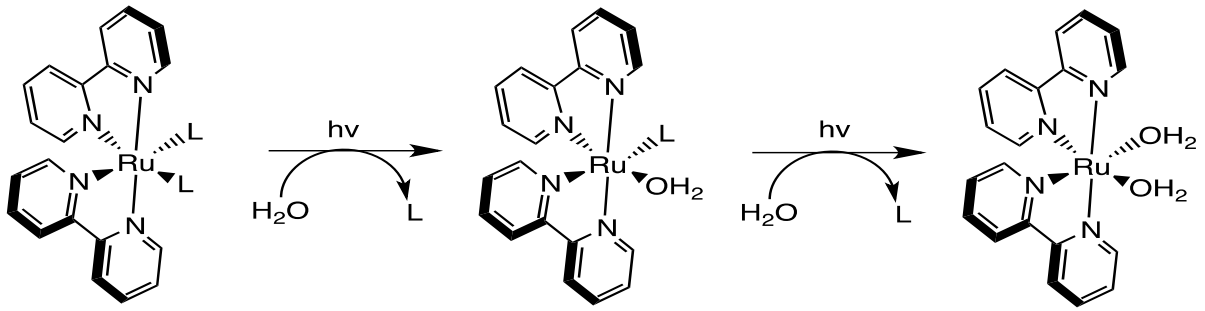

Figure 4. The mechanism of action of *cis*-$[Ru(bpy)_2(L)_2]^2$ (L = NH_3, pyridine, or CH_3CN). The bis-aqua species exchanges its water molecules for DNA-binding.

It has been shown in gel-electrophoresis studies that *cis*-$[Ru(bpy)_2(NH_3)_2]^{2+}$, *cis*-$[Ru(bpy)_2(py)_2]^{2+}$, and *cis*-$[Ru(bpy)_2(CH_3CN)_2]^{2+}$ inhibit the mobility of linear DNA when irradiated, but not in the dark, suggesting that these compounds indeed bind DNA upon photoactivation.[10,15,16] Efficient ligand exchange occurs with light that is the same energy as the light that the metal complex absorbs, which is typically in the visible region, on the border of the PDT window.[17] This requirement has led to the exploration and synthesis of polypyridyl ruthenium(II) complexes containing different ligands, which could alter the electronic properties of the compound and shift the absorption spectrum to lower energies, into the desired PDT window. Many of these ligands have extended π-systems (i.e. dpq, dppz, and dppn shown in **Figure 5**), which may also impart additional desirable qualities to the complex, such as dual-binding action through covalent DNA binding as well as DNA intercalation via the extended π-system.

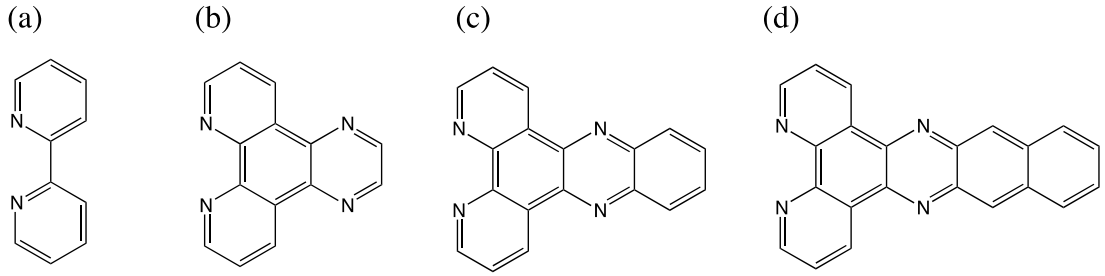

Figure 5. (a) bpy = 2,2'-bipyridine (b) dpq = dipyrido [3,2-f:2',3'-h]-quinoxaline **(c)** dppz = dipyrido [3,2-a:2',3'-c] phenazine **(d)** dppn = benzo[i]-dipyrido [3,2-a:2',3'-c] phenazine.

While many of these polypyridyl ruthenium(II) complexes are currently being studied, this work investigates ruthenium(II) complexes with cyclometallating ligands, which, like extended π-ligands, shift the absorbance toward red. Several cyclometallated ruthenium complexes have been shown to exhibit potent anti-tumor activity without many of the adverse side effects.18 The ligands present in the complexes studied in this work are shown below in **Figure 6**.

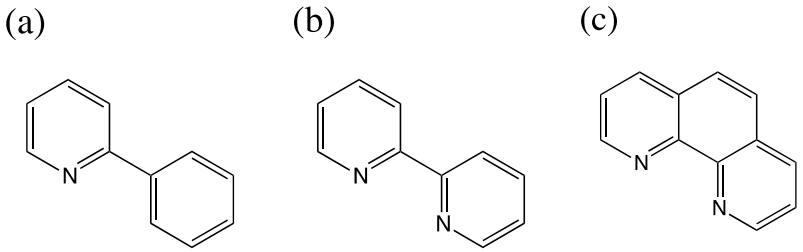

Figure 6. (a) $phpy^-$ = deprotonated 2-phenylpyridine; a cyclometallating ligand (b) bpy = 2,2'-bipyridine (c) phen = 1,10-phenanthroline.

1.4 CYCLOMETALLATED RUTHENIUM(II) COMPLEXES

The cyclometallated ruthenium(II) photo-cisplatin analog *cis*-$[Ru(phen)(phpy)(CH_3CN)_2]^+$ (**1**; phpy= 2-phenylpyridine) has been shown to inhibit the growth of tumors implanted in mice without severely impacting the hepatic, renal and nervous systems, all of which were observed to be impacted in mice treated with cisplatin.[18,19,20] Cell cycle analysis of the tumor cells treated with **1** revealed many cells to be arrested in the G0/G1 phase or undergoing apoptosis.[18] In subsequent studies, two groups of mice implanted with glioma cells were injected with either **1** or cisplatin; both treatments reduced the tumor size to nearly half the original size, suggesting comparable efficacy between the two treatments; however, mice treated with **1** suffered fewer side effects than mice treated with cisplatin.[18] Toxicity of the two treatments was evaluated over extended treatment: groups of mice were injected regularly with **1** or cisplatin over a three week period and changes in body mass were recorded; mice treated with **1** did not experience a significant decrease in body mass, while mice injected with cisplatin lost nearly one fourth of their body mass.[18] Blood analysis of these mice revealed that cisplatin-treated mice experienced altered levels of blood biomarkers indicative of abnormal renal and hepatic functioning, while mice treated with **1** did not experience these effects.[18] In additional studies, treatment of **1** together with ionizing radiation (IR) was tested against several tumor cell lines resulting in significant decreases in their proliferation.[19] The results described in these studies suggest that **1** and related compounds may possess the desired qualities of efficient PDT agents.

Despite the striking results of the aforementioned studies and the results from recent studies by Sears et. al., which found that Hs-27 skin cells and H2119 lung cancer cells treated with **1** experienced a nearly 3-fold increase in toxicity upon irradiation (LC_{50}^{dark} = 7.1 μM ;

LC_{50}^{irr} = 2.7 μM), the photoactivity of **1** was not measured (LC_{50} is the concentration of a drug required to kill 50% of the dosed population).[19] This nearly 3-fold increase in toxicity of **1** upon irradiation, is a value comparable to 5.5-fold increase in toxicity of the FDA-approved PDT agent porfimer sodium.[17] Additionally, complex **1** was found to undergo efficient ligand exchange when irradiated with light within the PDT window.[17] Complex **1** was also observed to decrease the mobility of linearized DNA upon irradiation, suggesting a DNA-binding mechanism for **1**. These qualities suggest that **1** and possible analogs may possess the desired photochemical and photophysical qualities of PDT agents. This work continues to investigate the photochemical properties of **1** and its analog **2**, $[Ru(phpy)(bpy)(CH_3CN)_2]^+$. Both complexes are shown in **Figure 7.**

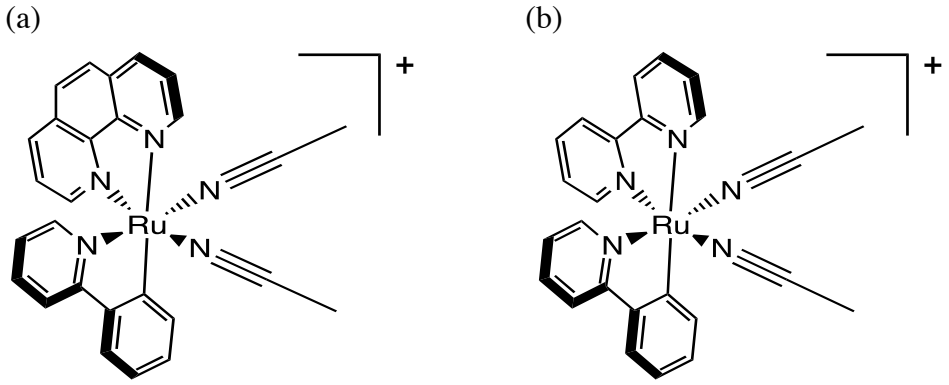

Figure 7. (a) **1** = $[Ru(phpy)(phen)(CH_3CN)_2]^+$ (b) **2** = $[Ru(phpy)(bpy)(CH_3CN)_2]^+$

It is important to note that both complex **1** and **2** contain the cyclometallating $phpy^-$ ligand, which extends the tail of the absorption profile of **1** and **2** into the PDT window, thereby making these complexes more practical as potential PDT agents. The lowest energy electronic transition of the previously described polypyridyl Ru(II) complexes with the general structure $[Ru(bpy)_2(L)_2]^{2+}$ (L = NH_3, pyridine, or CH_3CN) is from Ru→bpy, a transition, such that it is a metal to ligand charge transfer (MLCT). When an electron undergoes an MLCT transition, moving from the metal center to the bpy ligand, the complex is in a higher energy state and loss of the photolabile ligands can occur. This allows the Ru(II) complex to undergo ligand loss when irradiated and covalently bind DNA. Replacing one of the bpy ligands in $[Ru(bpy)_2(L)_2]^{2+}$ with a cyclometallating ligand such as $phpy^-$, as is the case in **1** and **2,** lowers the energy of the MLCT transition (Ru→bpy in **2** and Ru→phen in **1**) so that it falls into the ideal PDT window.[21]

1.5 THE ROLE OF GLUTATHIONE IN TOXICITY

Reduced glutathione (GSH) is one of the most abundant non-proteinaceous thiol-containing molecules in the cell and its structure is illustrated in **Figure 8.**[28] GSH functions primarily as an antioxidant molecule and is composed of the amino acids cysteine, glycine and glutamate. GSH reduces free radicals and reactive oxygen species such as H_2O_2 in order to lessen the oxidative stress.[22] GSH has been shown to coordinate in metal complexes containing zinc, lead, mercury, and cadmium metal centers.[23] Because GSH is involved in many biological reactions, has been shown to interact with transition metal complexes, and has a ubiquitous presence within the cell, its potential role in the generation of activated complexes of both **1** and **2** was investigated in this work.

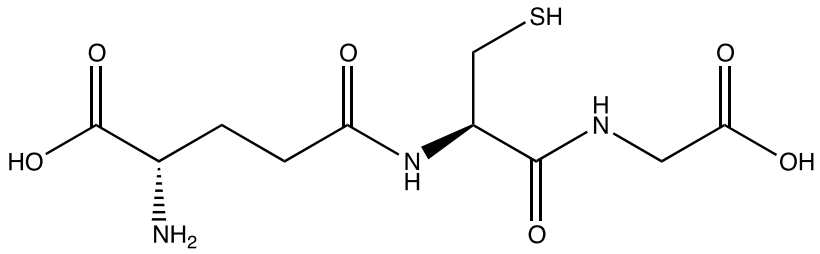

Figure 8. Reduced glutathione, composed of cysteine, glycine, and glutamic acid.

CHAPTER 2

EXPERIMENTAL METHODS

2.1 MATERIALS

L-Glutathione reduced (99%) was obtained from Sigma Aldrich and L-Glutathione oxidized (98%) was obtained from Acros Organics. The complex *cis*-[Ru(phpy)(bpy)(CH_3CN)$_2$](PF_6) (**2**) was synthesized by Bruno Peña according to a previously published procedure.[24] The complex *cis*-[Ru(phpy)(phen)(CH_3CN)$_2$](PF_6) (**1**) was synthesized by Maya Ojaimi following a previously published procedure.[17]

2.2 INSTRUMENTATION AND METHODS.

A Bruker MicroTOF spectrometer was used for electrospray ionization mass spectrometry (ESI-MS) measurements; Bruker Daltonics Data Analysis software version 3.4 was used to analyze ESI-MS measurements. Photolysis of **1** and was carried out in a borosilicate NMR tube placed at the focal point of a 150 W Xe arc lamp; a glass 1x1 cm cuvette was used for photolysis of **2**. The wavelength of irradiation for photolysis was controlled with a 455 nm long-pass glass filter placed in front of the light source. Absorption spectra were analyzed with a Hewlett Packard 8453 diode array spectrometer and Hewlett Packard 8453 Win System Software. ESI-MS studies and electronic absorbance spectra were performed in either a DMSO:H_2O solution or a CH_3CN:H_2O solution (33/66 or 1/99, v:v).

CHAPTER 3

RESULTS AND DISCUSSION

3.1 ELECTRONIC ABSORBANCE OF *cis*-[Ru(phpy)(bpy)(CH_3CN)$_2$](PF_6)

The ground state absorption spectra of **1** and **2** in CH_2Cl_2 measured in the dark by electronic absorption spectroscopy showed complexes **1** and **2** absorbing light in the visible and ultraviolet regions, an expected result in comparison to absorption spectra of similar cyclometallated ruthenium complexes.[21,25] In CH_2Cl_2, a ligand-centered $\pi\pi^*$ transition occurs for **2** at 295 nm (ε = 61,890 $M^{-1}cm^{-1}$) and for **1** at 267 nm (ε = 96,725 $M^{-1}cm^{-1}$).[25] These transitions are consistent with transitions observed at 293 nm (ε = 46,400 $M^{-1}cm^{-1}$) of the related complex $[Ru(phpy)(bpy)_2]^+$ in CH_3CN.[26] Also observed for $[Ru(phpy)(bpy)_2]^+$ in CH_3CN are absorption maxima at 369 nm (ε = 8,920 $M^{-1}cm^{-1}$) and 404 nm (ε = 8,230 $M^{-1}cm^{-1}$), which correspond to Ru→phpy$^-$ MLCT transitions;[21,25] Ru→bpy MLCT transitions were assigned to local maxima at 492 nm (ε = 6,480 $M^{-1}cm^{-1}$) and 546 nm (ε = 7,380 $M^{-1}cm^{-1}$).[21,25] Another related complex $[Ru(phpy)(CH_3CN)_4]^+$ exhibits Ru→phpy$^-$ MLCT transition at 380 nm.[24] Based on the absorption assignments of the related complexes $[Ru(phpy)(bpy)_2]^+$ and $[Ru(phpy)(CH_3CN)_4]^+$, the maxima observed for **2** at 372 nm (ε = 13,503 $M^{-1}cm^{-1}$) and for **1** at 396 nm (ε = 13,466 $M^{-1}cm^{-1}$) can be assigned to Ru→phpy$^-$ MLCT transition.[25,24,27] For **2**, the absorption maxima at 472 nm (ε = 8,480 $M^{-1}cm^{-1}$) and 479 nm (ε = 8,983 $M^{-1}cm^{-1}$) were assigned to the Ru→bpy MLCT transitions.[25] For **1**, Ru→phen the MLCT transitions were observed with maxima at 461 nm (ε = 11,559 $M^{-1}cm^{-1}$) and 486 nm (ε = 10,842 $M^{-1}cm^{-1}$).[25]

A low energy MLCT transition that extends beyond 600 nm and into the PDT window is also observed for both **1** and **2**, a critical feature for PDT agents.[25]

Irradiation of **2** (80 μM) with visible light in $CH_3CN:H_2O$ (1:99, v:v) resulted in changes in the absorption spectrum, suggesting that ligand exchange is occurring. The absorption spectrum is shown in **Figure 9**.

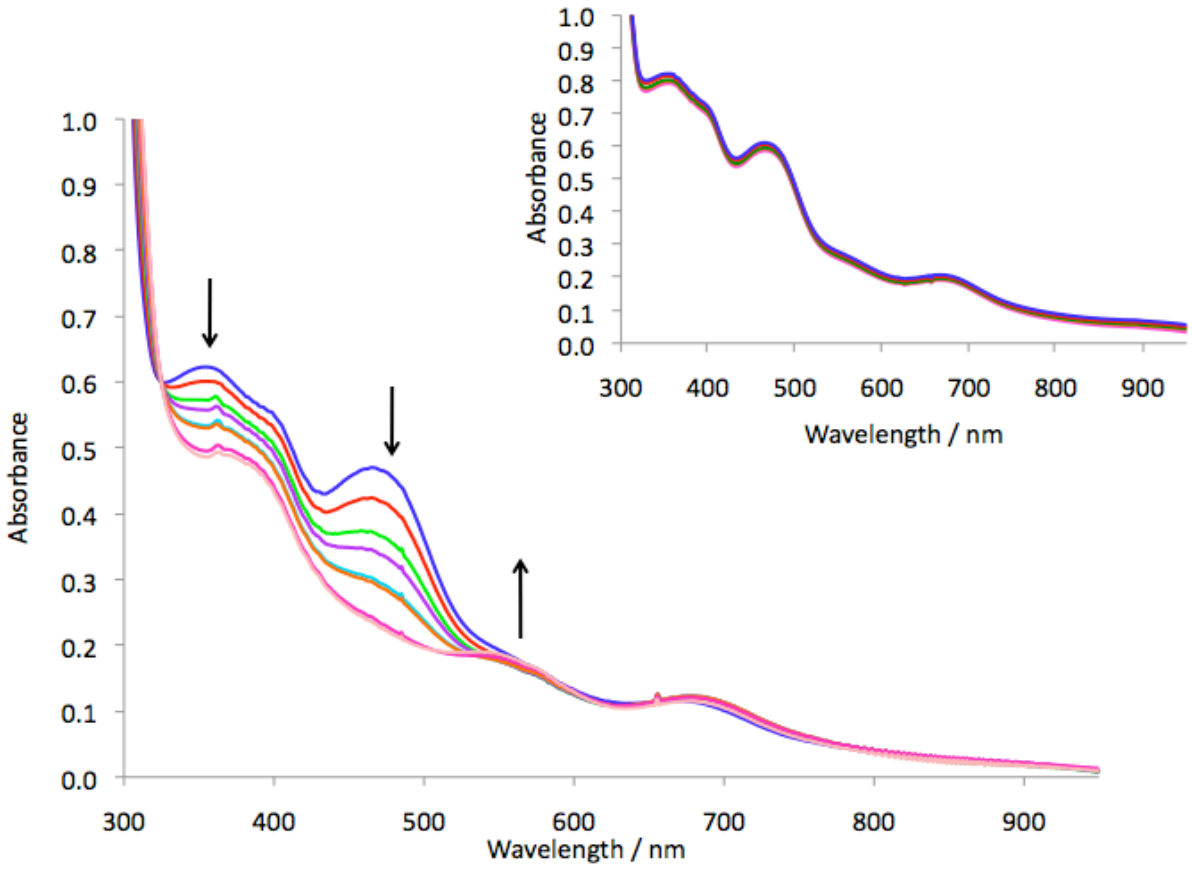

Figure 9. Changes in the electronic absorption spectrum of **2** (80 μM) as a function of irradiation time was measured in $CH_3CN:H_2O$ (1:99, v:v) at 0, 1, 2, 3, 4, 5, 10, 15 min. Inset: dark control over 45 min. Irradiation done with λ > 455 nm light.

The photolysis reaction of **2** in CH_3CN:H_2O (1:99, v:v) was also followed by ESI-MS with irradiation for 15 min ($\lambda > 475$ nm) (**Figure 10**). Before photolysis, the major species present include several species. Peak A (m/z = 494.0) corresponds to the parent ion $[Ru(phpy)(bpy)(CH_3CN)_2]^+$. A strong peak S (m/z = 440.0) is assigned to $[Ru(phpy)(CH_3CN)_4]^+$, an impurity that corresponds to the major starting material in the synthesis of **2**. Peak B (m/z = 453.0) is assigned to $[Ru(phpy)(bpy)(CH_3CN)]^+$. After irradiation for 15 min, **Figure 10b** demonstrates that the identities of peaks S and B do not change while the relative intensity of the parent ion peak A has decreased drastically with the emergence of the major photoproduct peak L (m/z = 429.1), which is assigned to $[Ru(phpy)(bpy)(H_2O)]^+$.

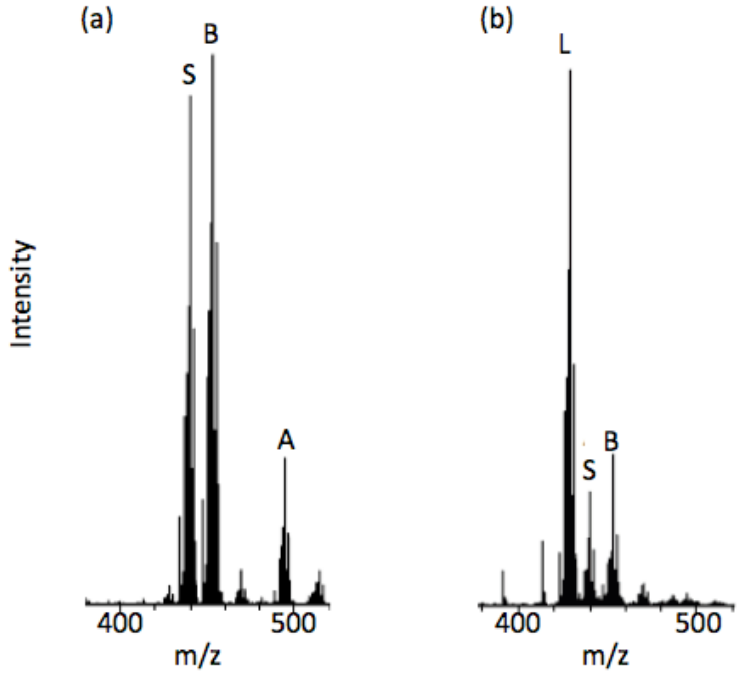

Figure 10. ESI-MS of **2** (80 μM) in a CH_3CN:H_2O (1:99, v:v) solution (a) before irradiation (b) after irradiation for 15 min ($\lambda > 475$ nm).

3.2 THE INTERACTION OF GSH WITH *cis*-[Ru(phpy)(bpy)(CH_3CN)$_2$](PF_6) AND *cis*-[Ru(phpy)(phen)(CH_3CN)$_2$](PF_6)

The electronic absorption profile of **2** incubated with GSH was measured over time in the dark in a 1% DMSO solution, shown in **Figure 11**, with the corresponding dark control (**Figure 11** inset). Upon mixing with GSH, the electronic absorption profile changes immediately with a general decrease in all the peaks of the starting material and the appearance a new band at 579 nm.

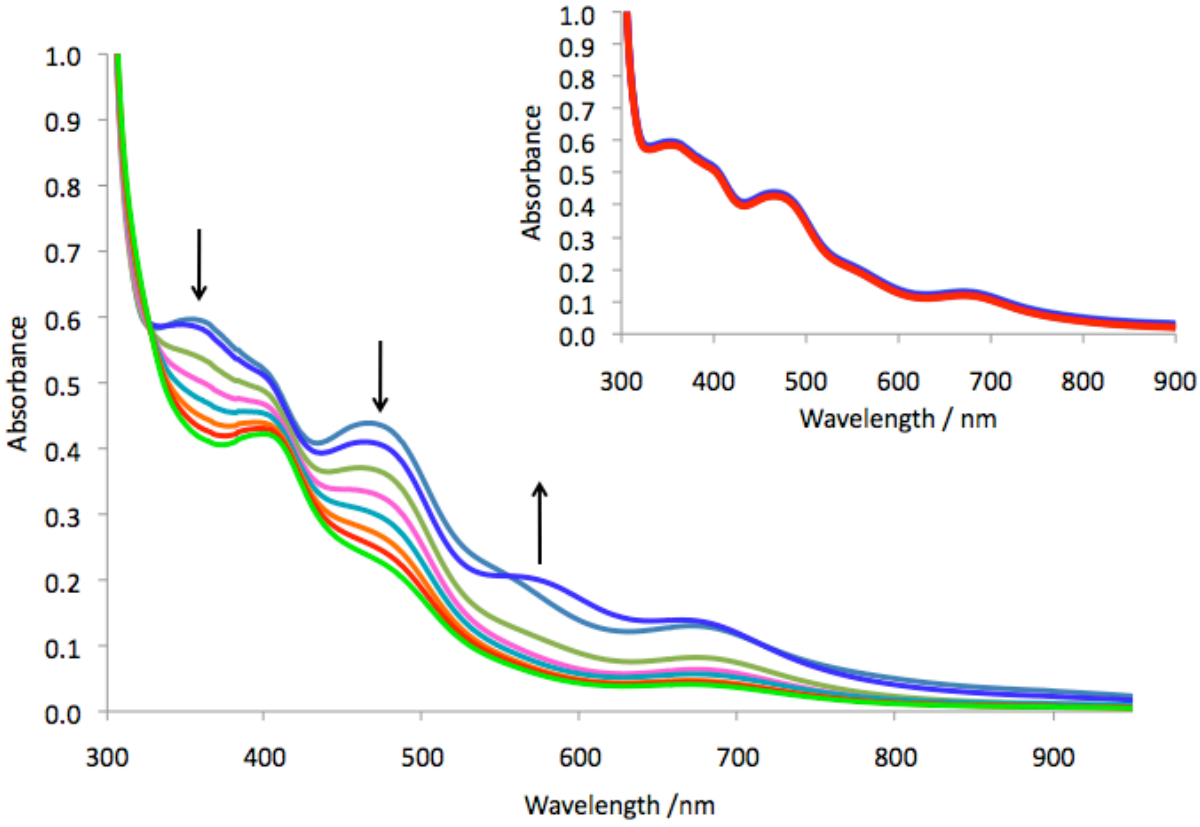

Figure 11. Changes in the electronic absorption spectrum of **2** (80 μM) after addition of 10 equivalents of GSH was measured in the dark as a function of incubation time with GSH in DMSO:H_2O (1:99, v:v) at 0, 1, 2, 3, 4, 5, 10, 15 min. Inset: dark control without GSH over 45 min.

Since **2** was observed to undergo ligand exchange in the presence of GSH, and because there is a high concentration of reduced glutathione (GSH) within the cell (0.5 mM – 10 mM GSH depending on the cell type), the possible role of GSH in contributing to the activation of **1** and **2** was investigated.[28] The ESI-MS spectrum of **1** (670 μM) in DMSO-d_6:D_2O (33:67, v:v), shows the peak denoted by A (m/z = 518.1) which corresponds to the parent ion of **1**, $[Ru(phpy)(phen)(CH_3CN)_2]^+$ (**Figure 12a**). A strong peak denoted by B (m/z = 477.1) corresponds to the complex with loss of one CH_3CN ligand, $[Ru(phpy)(phen)(CH_3CN)]^+$. **Figure 12b** illustrates that A and B are still the dominant peaks in the spectrum after 20 h in the dark at room temperature, suggesting that the complexes are stable; the emergence of a small amount of the DMSO-d_6-monosubstituted product $[Ru(phpy)(phen)(CH_3CN)(DMSO\text{-}d_6)]^+$ appears at the peak labeled C (m/z = 561.2). In **Figure 12c**, GSH was added to the sample from **Figure 12b** and ESI-MS was measured 20 min following the addition. Addition of GSH resulted in the relative increase of the DMSO-d_6-monosubstituted product, denoted by peak C (m/z = 561.2) (**Figure 12c**). A DMSO-d_6-disubstituted product, $[Ru(phpy)(phen)(DMSO\text{-}d_6)_2]^+$, in which both CH_3CN ligands are lost and two molecules of DMSO-d_6 are coordinated to the metal center, is denoted by D (m/z = 604.2). A peak denoted E (m/z = 577.2) also appeared and might correspond to the addition of a hydroxide to the product formed in C. Similar results were obtained for **2**. In **Figure 12d**, the peak A (m/z = 494.1) corresponds to the parent ion of **2**, $[Ru(phpy)(bpy)(CH_3CN)_2]^+$. A strong peak denoted by B (m/z = 453.1) corresponds to the ion with loss of one CH_3CN ligand, $[Ru(phpy)(bpy)(CH_3CN)]^+$. The levels of A and B remain stable after 20 h in the dark (**Figure 12e**). Upon addition of GSH, two new peaks emerge (**Figure 12f**). The addition of GSH results in an increase in the DMSO-d_6-

monosubstituted product $[Ru(phpy)(bpy)(CH_3CN)(DMSO\text{-}d_6)]^+$ denoted by peak C (m/z = 537.2), as well as the DMSO-d_6-disubstituted product $[Ru(phpy)(bpy)(DMSO\text{-}d_6)_2]^+$ denoted by peak D (m/z = 580.2). The results presented below in **Figure 12** demonstrate that GSH facilitates ligand loss from both **1** and **2** in exchange for coordination by DMSO-d_6 molecules.

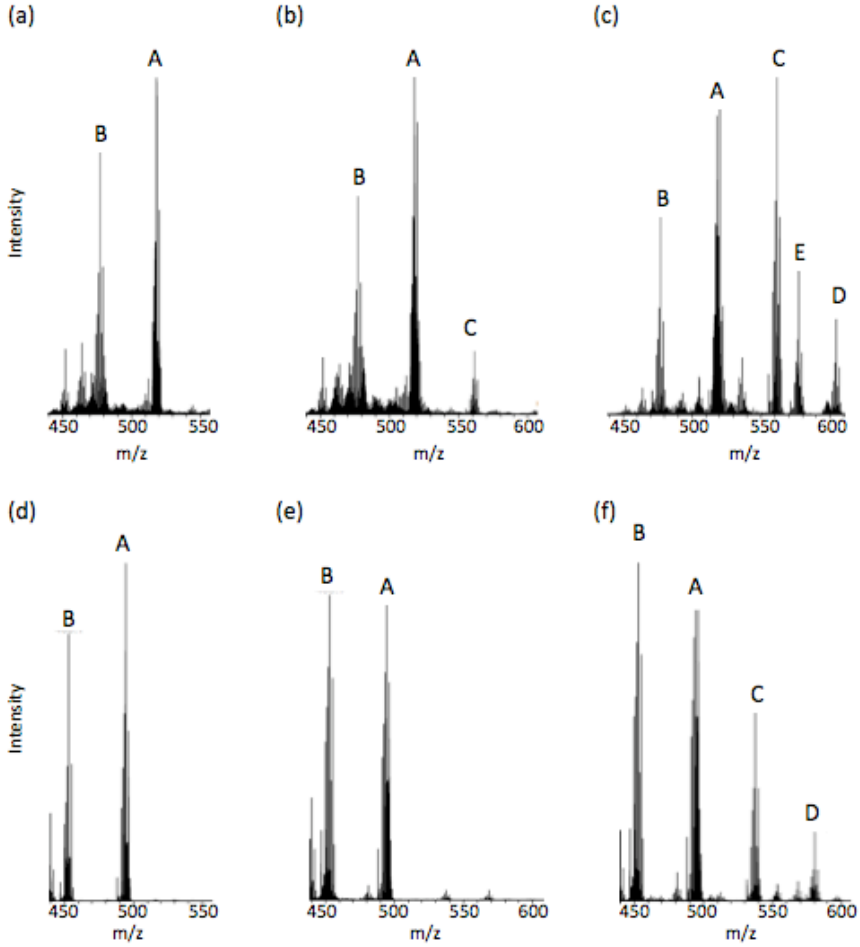

Figure 12. ESI-MS of **1** (670 μM) (a)–(c) and of **2** (670 μM) (d)-(f) in DMSO-d_6:D_2O (33:67, v:v) (a) and (d) correspond to time 0, immediately after addition of the ruthenium complexes to the DMSO-d_6:D_2O solution. (b) and (e) were measured after 20 h in the dark at room temperature. (c) and (f)

were measured 20 min after 10 equivalents of GSH were added to the respective samples described in (b) and (e).

In an *in vivo* environment, such interaction between GSH and either **1** or **2** may result in ligand exchange and subsequent covalent binding to DNA in lieu of coordination by DMSO-d_6 molecules. The ESI-MS shown in **Figure 13** demonstrates the changes that occur when **1** is incubated for 20 h in the dark with GSH, or to a much lesser extent, with GSSG.

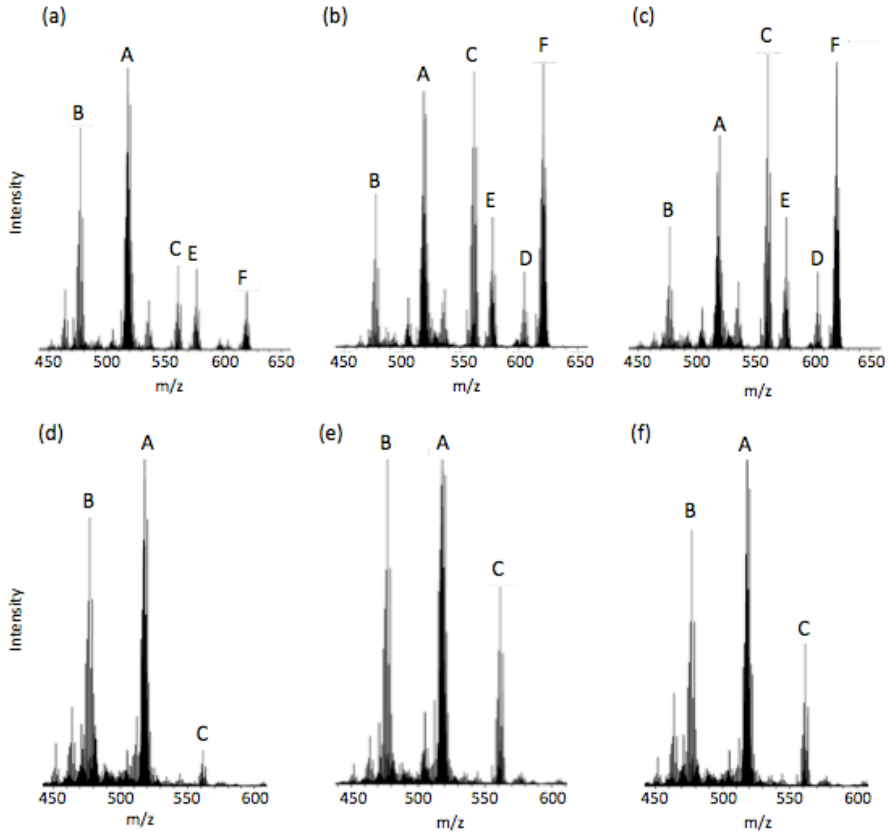

Figure 13. ESI-MS of **1** (670 μM) in DMSO-d_6:D_2O (33:67, v:v) (a) immediately after addition of 10 equivalents of GSH to **1** in the DMSO-d_6:D_2O solution (b) after 20 h in the dark at room temperature (c) after 30 min of irradiation ($\lambda > 455$ nm). ESI-MS of **1** (670 μM) in DMSO-d_6:D_2O (33:67,

v:v) (d) immediately after addition of 5 equivalents of GSSG to **1** in the DMSO-d_6:D_2O solution (e) after 20 h in the dark at room temperature (f) after 30 min of irradiation.

Figure 13a illustrates the spectrum of **1** incubated with GSH immediately after mixing. The DMSO-d_6-substituted products C, E, and F are present. After 20 h in the dark, the DMSO-d_6-disubstituted product D appears, and the relative intensities of C, E, D, and F increase in comparison with the parent ion, A (**Figure 13b**). Peak F corresponds to product D with an added hydroxide or oxygen atom. After irradiation, the identities of the products present does not change in comparison with the spectrum obtained before irradiation; however, it is possible that irradiation triggered isomerization of the DMSO molecule in DMSO-coordinated species (**Figure 14**). Such isomerization of the DMSO molecule from S-bound to O-bound form is known to occur upon irradiation (**Figure 14**).[29,30]

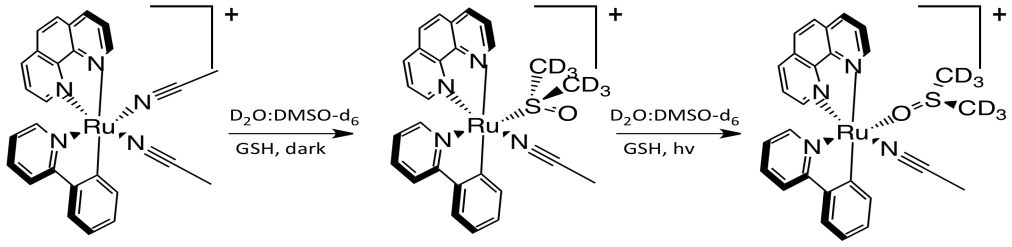

Figure 14. Irradiation of the DMSO-d_6-monosubstituted species $[Ru(phpy)(phen)(CH_3CN)(DMSO\text{-}d_6)]^+$ is thought to lead to isomerization of the DMSO molecule from S-bound to O-bound.

Because GSH is oxidized to the disulfide dimer GSSG in the presence of DMSO, it was necessary to assess the effect of GSSG on **1** under both dark and irradiated conditions.[31] In **Figure 13d** and **13e**, 670 μM of **1** was incubated with 5 equivalents of GSSG in a DMSO-d_6:D_2O solution for 20 h at room temperature in the dark. A comparison between initial mixing of **1** and GSSG with **Figure 13e** 20 h later reveals an increase in the relative intensity of the monosubstituted product C $[Ru(phpy)(phen)(CH_3CN)(DMSO\text{-}d_6)]^+$, while the intensity of the parent ion A does not change significantly. Subsequent photolysis of the sample does not have a noticeable effect on the ESI-MS spectrum (**Figure 13f**).

Similar results were obtained for **2**. In **Figure 15**, it is first important to note that peak S (m/z = 440.0), which is present in all spectra of Figure 13, is the impurity $[Ru(phpy)(CH_3CN)_4]^+$, the starting material used in the synthesis of **2**; the peak corresponding to product I (m/z = 456.1) is a photoproduct of the starting material and corresponds to $[Ru(phpy)(CH_3CN)_4]^+$ with two associated solvent water molecules. Further discussion will focus on products generated from **2** and not on peaks corresponding to starting reagents. **Figure 15** illustrates that **2** indeed interacts with GSH in a manner similar to the interaction observed for **1**. In the ESI-MS spectrum of **1** (665 μM) mixed with 10 equivalents of GSH in DMSO:H_2O (33:67, v:v), the peak denoted by A (m/z = 494.1) corresponds to the parent ion $[Ru(phpy)(bpy)(CH_3CN)_2]^+$ (**Figure 15a**). A strong peak denoted by B (m/z = 453.1) corresponds to the complex with loss of one CH_3CN ligand, $[Ru(phpy)(bpy)(CH_3CN)]^+$ that is due to ionization. The relatively low intensity peak D (m/z = 567.0) corresponds to the small presence of a DMSO-disubstituted product $[Ru(phpy)(bpy)(DMSO)_2]^+$. Peak E (m/z = 613.1) corresponds to oxidized glutathione, GSSG. **Figure 15b** demonstrates that after 20 h in the dark at room temperature, both the

parent ion peak A and peak B are absent, while peak E has grown in relative intensity suggesting that much of the parent ion has reacted. Additionally, a range of DMSO-coordinated products emerges. The strong peak F (m/z = 490.0) corresponds to a DMSO-monosubstituted product $[Ru(phpy)(bpy)(DMSO)]^+$. Peak G (m/z = 506.0) corresponds to $[Ru(phpy)(bpy)(DMSO)(H_2O)]^+$. Peak C (m/z = 531.0) corresponds to a DMSO-monosubstituted product $[Ru(phpy)(bpy)(CH_3CN)(DMSO)]^+$. Peak J (m/z = 584.0) may correspond to the DMSO-disubstituted product $[Ru(phpy)(bpy)(DMSO)_2]^+$ associated with a solvent water molecule. In **Figure 15c**, the most noticeable change upon photolysis is that the intensities decrease due to the high relative intensity of E, which is GSSG (m/z = 613.0). However, photolysis does also result in the disappearance of the DMSO-monosubstituted product $[Ru(phpy)(bpy)(CH_3CN)(DMSO)]^+$ which corresponds to peak C, and the concomitant increase in the relative intensity of peak D, the DMSO-disubstituted product $[Ru(phpy)(bpy)(DMSO)_2]^+$. While the disappearance of the analogous peak was not observed for **1**, it is possible that **2** is more reactive than **1**. This greater reactivity of **2** is observed in **Figure 15d-e** in which reactions occur in the presence of GSH in the dark and following irradiation. In **Figure 15d** and **15e**, 665 μM of **2** was incubated with 5 equivalents of GSSG in a DMSO:H_2O solution initially and for 20 h at room temperature in the dark, respectively. A comparison of the ESI-MS spectra reveals a decrease in the relative intensity of product B $[Ru(phpy)(bpy)(CH_3CN)]^+$ and a disappearance of the parent ion A after 20 h in the dark. A strong peak F corresponding to a DMSO-monosubstituted product and product C also emerge. Photolysis of **2** in the presence of GSSG results in the disappearance of peak C and the increase in the relative intensity of peak D, otherwise the identities of the photoproducts do not differ from the products in **Figure 15e**. **Figure 15** of **2** in the presence of either GSH

or GSSG clearly shows that ligand exchange and the generation of different DMSO or solvent coordinated products is less affected by the presence of GSH for **2** than for **1**; however, **2** more readily achieves different substitution products in the presence of GSH than in the presence of GSSG, suggesting that GSH may play a role in facilitating ligand exchange. Furthermore, it is worth noting that even the starting material impurity, corresponding to peak S, achieves a different product I, in the presence of GSH, but not in the presence of GSSG (**Figure 15**).

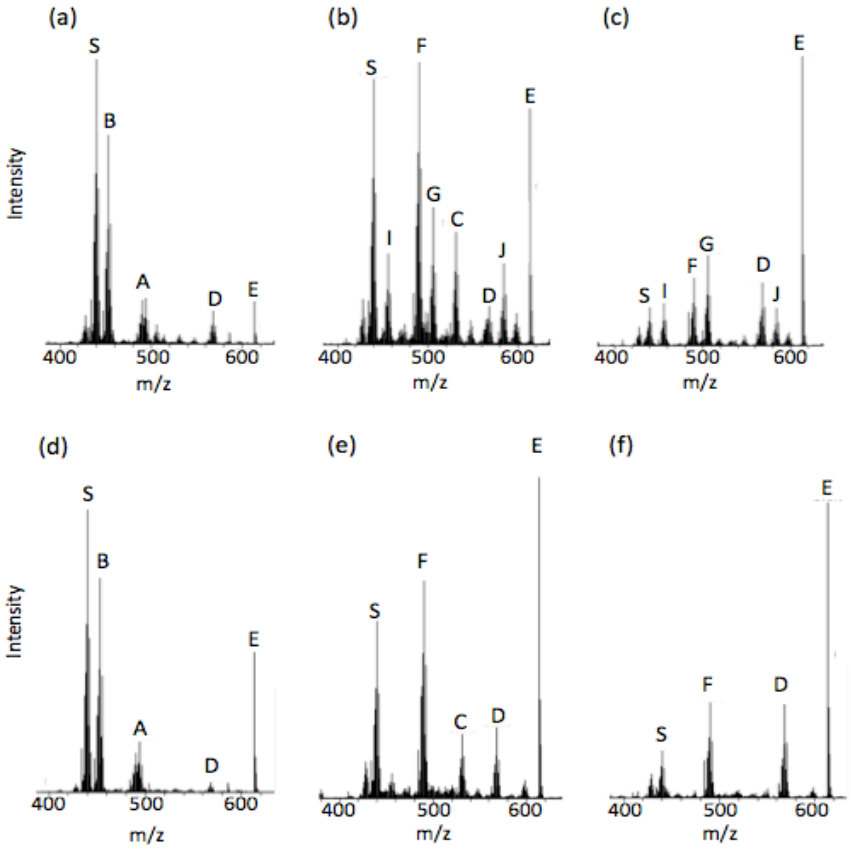

Figure 15. ESI-MS of **2** (665 μM) in DMSO:H_2O (33:67, v:v) (a) immediately after addition of 10 equivalents of GSH to **2** in the DMSO:H_2O solution (b) after 20 h in the dark at room temperature (c) after 30 min of irradiation ($\lambda > 455$ nm). ESI-MS of **2** (665 μM) in DMSO:H_2O (33:67, v:v)

(d) immediately after addition of 5 equivalents of GSSG to **2** in the DMSO:H_2O solution (e) after 20 h in the dark at room temperature (f) after 30 min of irradiation.

CHAPTER 4

CONCLUSION AND REFERENCES

4.1 CONCLUSION

The present work illustrates that the ruthenium(II) cyclometallated complexes of **1** and **2** have electronic absorption profiles that are shifted to lower energy wavelengths and into the PDT window. Upon irradiation, both **1** and **2** undergo ligand dissociation and coordination by solvent molecules (DMSO or H_2O). Additionally, experiments conducted with GSH suggest that GSH interacts with both **1** and **2** to facilitate ligand exchange in both dark and irradiated conditions. The phototoxicity of **1** toward tumor cells in mouse models as well as toward cell lines may result from both photoinduced and GSH-induced ligand exchange.[18,17] Due to the presence of DMSO in stock solutions used to solubilize **1** for cell viability assays, it is possible that a DMSO-coordinated species may play a role in the observed cytotoxicity toward tumor cell lines.[29,25] Future work should address further characterizing the interaction between GSH and complexes **1** and **2**.

4.2 REFERENCES

[1] Astolfi, L., Ghiselli, S., Guaran, V., Chicca, M., Simoni, E., Olivetto, E., Lelli, G., Martini, A. 2012. Correlation of adverse effects of cisplatin administration in patients affected by solid tumours: A retrospective evaluation. *Oncology Reports*. (DOI: 10.3892/or.2013.2279)

[2] Scwingel, A. R., Barcessat, A. R. P., Núñez, S. C., Ribeiro, M. S. 2012. Antimicrobial Photodynamic Therapy in the Treatment of Oral Candidiasis in HIV-infected Patients. *Photomedicine and Laser Surgery*. **30** 429-432 (DOI: 10.1089/pho.2012.3225)

[3] Sharma, S. K., Mroz P., Huang Y. Y., St Denis, T. G., Hamblin M. R. 2012. Photodynamic Therapy for Cancer and for Infections: What Is the Difference? *Isr J Chem*. **52** 691-705 (DOI: 10.1002/ijch.201100062)

[4] Sternberg, E., Dolphin, D.; Brückner, C. 1998. Porphyrin-based Photosensitizers for Use In Photodynamic Therapy. *Tetrahedron*. **54** 4151-4202

[5] Patrice, T., Moan, J., Peng, Q. 2003 An Outline of the History of PDT. *Photodynamic Therapy*. 9-10 (DOI: 10.1039/9781847551658-00001)

[6] Yue, X., Yanez C. O., Yao, S., Belfield, K. 2013. Selective Cell Death by Photochemically Induced pH Imbalance in Cancer Cells. *J. Am. Chem*. **135,** *6* 2112-2115 (DOI: 10.1021/ja3122312)

[7] O'Connor, A. E., Gallagher, W. M. and Byrne, A. T. 2009 Porphyrin and Nonporphyrin Photosensitizers in Oncology: Preclinical and Clinical Advances in Photodynamic Therapy. *Photochem. Photobiol*. **85**, 1053-1074. (DOI 10.1111/j.1751 - 1097.2009.00585.x)

[8] Lutterman, D. A., Fu, P. K. and Turro, C. 2006 cis-[Rh2(μ-O_2CCH_3)$_2$(CH_3CN)$_6$]$^{2+}$ as a Photoactivated Cisplatin Analog. *J. Am. Chem. Soc. Comm.* **128**, 738-739. (DOI 10.1021/ja057620q)

[9] Garner, R., Gallucci, J., Dunbar, K. R. and Turro, C. 2011 [Ru(bpy)$_2$(5-cyanouracil)$_2$]$^{2+}$ as a Potential Light-Activated Dual-Action Therapeutic Agent. *Inorg. Chem.* **50**, 9213-9215. (DOI 10.1021/ic201615u)

[10] Singh, T. and Turro, C. 2004. Photoinduced DNA Binding by a Ru(II) Complex: A photo-cisplatin analog. *Inorg. Chem.* **43**, 7260-7262. (DOI 10.1021/ic049075k)

[11] Toney, J. H., Donahue, B. A., Kellett, P. J., Bruhn, S. L., Essigmann, J. M., Lippard, S. J. 1989. Isolation of cDNAs enconding a human protein that binds selectively to DNA modified by the anticancer drug *cis*-diammine-dichloroplatinum(II). *Proc. Natl. Acad. Sci.* **86** 8328-8332 (PMID:2530581)

[12] Burya, S. J., Palmer, A. M., Gallucci, J. C., Turro, C. Photoinduced Ligand Exchange and Covalent Binding by Two New Dirhodium Bis-Amidato Complexes. *Inorg Chem.* **51** 11882-11890 (DOI 10.1021/ic3017886I)

[13] Puim, D., van Waardenburg, R. C., Beijnen, J. H. and Schellens, J. H. 2004 Cytotoxicity of the organic ruthenium anticancer drug NAMI-A is correlated with DNA binding in four different human tumor cell lines. *Cancer Chemother. Pharmacol.* **54**, 71-78. (DOI 10.1007/s00280-004-0773-6)

[14] Hartinger, C. G., Zorbas-Seifried, S., Jakupec, M. A., Kynast, B., Zorbas, H. and Keppler, B. K. 2006 From bench to bedside - preclinical and early clinical development of the anticancer agent indazolium trans-[tetrachlorobis(1H-indazole)ruthenate(III)]

(KP1019 or FFC14A). *J. Inorg. Biochem.* **100**, 891-904. (DOI 10.1016/j.jinorgbio.2006.02.013)

[15] Pinnick, D. V., Durham, B. 1984. Photosubstitution reactions of Ru(bpy)2XYn+ complexes. *Inorg. Chem.* **23** *10* 1440-1445 (DOI: 10.1021/ic00178a028)

[16] Liu, Y., Turner, D. B., Singh, T. N., Angeles-Boza, A. M., Chouai, A., Dunbar, K. R., Turro, C. 2009. Ultrafast ligand exchange: detection of a pentacoordinate Ru(II) intermediate and product formation. *J. Am. Chem. Soc. 131*, 26-27 (DOI: 10.1021/ja806860w)

[17] Sears, B. R., Joyce, L. E., Ojaimi, M., Gallucci. J. C., Thummel, R.P., Turro, C. 2012. Photoinduced ligand exchange and DNA binding of *cis*-$[Ru(phpy)(phen)(CH_3CN)_2]^+$ with long wavelength visible light. *J. Inorg. Biochem.* **121** 77-87 (DOI: 10.1016/j.jinorgbio.2012.12.003)

[18] Gaiddon, C., Jeannequin, P., Bischoff, P., Pfeffer, M., Sirlin, C., Loeffler, J. P. 2005. Ruthenium (II)-Derived Organometallic Compounds Induce Cytostatic and Cytotoxic Effects on Mammalian Cancer Cell Lines through p53-Dependent and p53-Independent Mechanisms. *J. Pharmacology and Therap.* **315** 1403-11 (DOI: 10.1124/jpet.105.089342)

[19] Leyva, L., Malek, F., Benzina, S., Denis, J. M., Gueulette, J., Dufour, P., Gaiddon, C., Loeffler, J. P., Sirlin, C., Pfeffer, M., Bischoff, P. 2008. Evaluation of the Ability of an Organic Derivative of Ruthenium(II) to Reinforce the Cytotoxicity of Fast Neutron Against Malignant Cells in Culture. *Letters in Drug Design & Discovery*. **5** 1-6 (doi: 10.2174/10001)

[20] Meng, Xiangjun; Leyva, Mili L.; Jenny, Marjorie; Gross, Isabelle; Benosman, Samir; Fricker, Bastien; Harlepp, Sebastien; Hebraud, Pascal; Boos, Anne; Wlosik, Pauline; Bischoff, Pierre; Sirlin, Claude; Pfeffer, Michel; Loeffler, Jean-Philippe; Gaiddon, Christian. 2009. A Ruthenium-Containing Organometallic Compound Reduces Tumor Growth through Induction of the Endoplasmic Reticulum Stress Gene *CHOP*. *Cancer Research*. 69 5458-5466.

[21] Bomben, P. G., Robson, K. C. D., Sedach, P. A. and Berlinguette, C. P. 2009. On the Viability of Cyclometalated Ru(II) Complexes for Light-Harvesting Applications. *Inorg. Chem.* **48**, 9631-9643. (DOI 10.1021/ic900653q)

[22] Presnell, C. E., Bhatti, G., Numan, L.S., Lerche, M., Alkhateeb, S. K., Ghalib, M., Shammaa, M., Kavdia, M. 2013. Computational Insights into the Role of Glutathione in Oxidative Stress. *Curr Neurovasc Res*. (Epub) PMID:23469953

[23] Fuhr BJ, Rabenstein DL. Nuclear Magnetic Resonance Studies of Solution Chemistry of Metal Complexes. IX. 1973. The Binding of Cadmium, Zinc, Lead and Mercury by Glutathione. *J Am Chem Soc* **95** *21* 6944-50 (DOI: 10.1021/ja00802a013)

[24] Ryabov, A. D., Le Lagadec, R., Estevez, H., Toscano, R. A., Hernandez, S., Alexandrova, L., Kurova, V. S., Fischer, A., Sirlin, C. and Pfeffer, M. 2005 Synthesis, Characterization, and Electrochemistry of Biorelevant Photosensitive Low-Potential Orthometalated Ruthenium Complexes. *Inorg. Chem.* **44**, 1626-1634. (DOI 10.1021/ic048270w)

[25] Palmer, A. M., Peña, B., Sears, B., Chen, O., Ojaimi, M., Thummel, R. P., Dunbar, K., R.,

Turro, C. Cytotoxicity of Cyclometallated Ruthenium Complexes: The Role of Ligand Exchange on the Activity. 2012. *Phil Trans A* (in press)

[26] Peña, B., Leed, N. A., Dunbar, K. R. and Turro, C. 2012 *J. Am. Chem. Soc*. Submitted.

[27] Ryabov, A. D., Estevez, H., Alexandrova, L., Pfeffer, M. and Le Lagadec, R. 2006 Unusual phenomenon in the chemistry of orthometalated ruthenium (II) complexes. *Inorganica Chimica Acta* **359**, 883-887. (DOI 10.1016/j.jca.2005.05.034)

[28] Reed, D. J., Fariss, M. W. 1984. Glutathione Depletion and Susceptibility. *Pharmacol. Rev*. **36** *2*, 25S – 33S. (PMID: 6382355)

[29] Lutterman, D. A., Rachford, A. A., Rack, J. J. and Turro, C. 2010 Electronic and Steric Effects on the Photoisomerization of Dimethylsulfoxide Complexes of Ru(II) Containing Picolinate. *The Journal of Physical Chemistry L*. **1**, 3371-3375. (DOI 10.1021/jz1012966)

[30] McClure, B. A. and Rack, J. J. 2010 Isomerization in Photochromic Ruthenium Sulfoxide Complexes. *European Journal of Inorganic Chem*. **25**, 3895-3904. (DOI 10.1002/ejic.200900548) (c) Rack, J. J. and Mockus, N. V. 2003 Room-Temperature Photochromism in *cis*- and *trans*-$[Ru(bpy)_2(dmso)_2]^{2+}$. *Inorg. Chem*. **42**, 5792-5794.

[31] Svardal, A. M., Mansoor, M. A. and Ueland, P. M. 1990. Determination of Reduced, Oxidized, and Protein-bound Glutathione in Human Plasma and Human Precolumn Derivatization with Monobromobimane and Liquid Chromatography. *Anal. Biochem*. **184**, 338-346.